THE BI-MODAL PATTERN OF THE SUMMER CIRCULATION OVER SOUTH AMERICA

Dirceu Luis Herdies[1*]
Arlindo da Silva[2]
Maria A. F. Silva Dias[3]

[1]Goddard Earth Sciences and Technology Center
University of Maryland, Baltimore County
NASA GSFC Data Assimilation Office Branch
Greenbelt, MD 20771 USA

[2]Data Assimilation Office
Nasa/Goddard Space Flight Center
Greenbelt, MD 20771 USA

[3]Institute of Astronomy and Geophysics
University of Sao Paulo
Sao Paulo, Brazil

Journal of Geophysical Research
Submitted to the special issue on LBA
06/20/2001

[*]Permanent Affiliation: Centro de Previsao de Tempo e Estudos Climaticos, Instituto Nacional de Pesquisas Espaciais, Rodovia Presidente Dutra km 40, Cachoeira Paulista, SP, Brazil. E-mail:dirceu@dao.gsfc.nasa.gov

ABSTRACT

Submonthly variations in warm-season (January-February) precipitation over South America, in special over the Amazon basin, central southwest Brazil, north Argentina, and Paraguay are shown to be strongly linked to variations in the moisture entering the continent from the Atlantic ocean. Two distinct regimes of lower tropospheric winds (westerlies and easterlies) were observed in Rondonia during the Wet Season Atmospheric Mesoscale Campaign (WETAMC) component of the Large Scale Atmosphere-Biosphere Experiment in Amazonia (LBA) and the Tropical Rainfall Measuring Mission (TRMM) field campaign. The westerly (easterly) winds were associated with the strong (weak) convective activity over the South Atlantic Convergence Zone (SACZ). The whole period of this study (January-February) was divided into SACZ and NSACZ (No SACZ) events. The vertically integrated moisture fluxes over the Amazon and Prata basin from the National Aeronautics and Space Administration/Goddard Data Assimilation Office (NASA/DAO) assimilation show that during SACZ (NSACZ) event strong (weak) convergence occurred over the Amazon basin with divergence (convergence) over the Prata basin. Submonthly variations in the SACZ also can be linked to extreme climate anomalies such as droughts or flooding conditions over the Amazon and Prata basin.

1 INTRODUCTION

Moisture plays a key role in several aspects of human life such as water supplies for daily needs and agriculture. The water balance of the Amazon basin is of great importance, due to the presence of one of world's largest hydrographic system. The Amazon region is an important source of heat and water vapor for the atmosphere and plays a significant role in the general circulation of the atmosphere (Garstang and Fitzjarrald 1999).

There is increasing recognition of the importance of the role played by moisture transport from the Amazon basin to extra tropical latitudes (Southern Brazil, Paraguay and Northern Argentina). The central and southern Amazon exhibits the largest integrated moisture convergence, especially during summer. Most of the annual total rainfall over the region occurs during the austral summer (December to February). The Tropical Atlantic region is the largest moisture source for the Amazon basin. Conversely, the Amazon region is a moisture source for other regions outside the Amazon (Marengo 2000).

Several authors have analyzed the variability of the summertime atmospheric circulation over subtropical South America from the viewpoint of interannual and interdecadal timescales (Robertson and Mechoso 2000). Relatively few studies have tried to understand the submontlhy variability and its three-dimensional structure and its relationship to the large scale circulation during the austral summer.

Incursion of tropical air into midlatitudes occurs on the eastern side of the Andes in two preferred regions. The first is located on subtropical latitudes, on the lee of the Andes near 20^{o}-30^{o}S, and the second is a function of the position of the South Atlantic Convergence Zone (SACZ), ocurring more the middle of the continent. The importance of the meridional air mass transport between tropical and extra tropical latitudes of South America is evident in the precipitation and surface temperature fields (Seluchi and Marengo 2000). The incursion of tropical air into the midlatitudes seems to be linked to the Chaco Low in northern Argentina and to the Atlantic subtropical high. Northerlies occurs in a narrow low-level jet east of the Andes that brings warm and moist air from the Amazon basin to the Prata river (northern Argentina, Paraguay and southern Brazil).The SACZ is a dominant summertime cloudiness feature of subtropical South America and adjacent south Atlantic Ocean. Normally, the SACZ is a cloud band that appears to either emanate from or merge with the intense convection over the Amazon basin, extending from the tropical South America southeastward into the South Atlantic Ocean (Kodama 1992, 1993; Figueroa et al. 1995; Nogués-Peagle and Mo 1997; Liebmann et al 1999; Robertson and Mechoso 2000)

The Wet Season Atmospheric Mesoscale Campaign (WETAMC) component of the Large Scale Atmosphere-Biosphere Experiment in Amazonia (LBA) and the Tropical Rainfall Measuring Mission (TRMM) field campaign, known as TRMM/LBA, were conducted in the southwest corner of the Amazon basin during the wet season months of January and February 1999 (Fig. 1). The goal of the field campaigns was to provide a detailed study of tropical convection in Amazonia, with its different impacts, as well as on the regional response to the larger scale forcing. Together, the WETAMC/LBA and TRMM/LBA campaigns represent an opportunity to study tropical convection in Amazonia and its relation to the underlying forested and deforested regions (Silva Dias et al. 2000).

The combined use of observations and modeling is a powerful tool to understanding the role of the moisture budget in this region and can improve the simulation and seasonal prediction of the climate anomalies. In this paper, we examine how the summer circulation over South America presents a bi-modal pattern with characteristic dry and wet periods. Section 2 describes the DAO/NASA analysis data set used in this study, and section 3 identifies the bi-modal pattern of the circulation observed over South America during the WETAMC/TRMM-LBA campaign. Results are discussed and summarized in section 4.

2 DATA AND METHODOLOGY

Four times daily analyses of wind velocity, specific humidity and moisture flux were obtained from Data Assimilation Office (DAO) at the National Aeronautic and Space

Administration (NASA) Goddard Space Flight Center for January and February 1999. For this study we use version 2 of the Goddard Earth Observing System (GEOS-2) Data Assimilation System (DAS). This system addresses many of the shortcomings in GEOS-1 DAS (Schubert et al. 1993), including improved vertical resolution and a global Physical-space Statistical Analysis System (PSAS). A detailed description of GEOS-2 is given in DAO (1996). The global data are available on a horizontal resolution of 2.5^{o} X 2.0^{o} latitude-longitude grid at 28 pressure levels. For the purposes of this study, the geographic domain is restricted to South America (20^{o}N-50^{o}S, 90^{o}W-20^{o}W).

Figure 1 deputs the enhanced WETAMC/TRMM-LBA experimental area in the State of Rondonia. The top panel shows the GTS (Global Telecommunication System) sites where radiosondes data are available on a routine basis to be assimilated into a global model. The colors means the number of radiosondes launched per site during January 1999. The closest data, of the experiment, used by GEOS-2 assimilation were Porto Velho (top of enhanced map) and Vilhena (bottom of enhanced map). The sounding data from ABRACOS (10^{o}46'S-62^{o}20'W, 290 MSL) were used as independent verification of the GEOS-2 assimilation, which did not include the WETAMC/TRMM-LBA field campaign data. The quality of the reanalysis dataset has been shown to be adequate in several studies of tropical and subtropical intraseasonal variability (Liebmann et al. 1999).

Daily Outgoing Longwave Radiation (OLR) from NOAA-CIRES/Climate Diagnostics Center (CDC) are used as proxies of tropical convection. This dataset has been interpolated to remove gaps due to missing values. The daily values represent averages of the day and night passes of the polar-orbiting satellites (Liebmann and Smith 1996).

The site of ABRACOS was chosen because it represents the longest intensive observing period during WETAMC/TRMM-LBA campaign. The radiosondes were launched at approximately three hour intervals, for the period from 9 January until 28 February 1999 (Silva Dias et al 2001). A total of about 317 soundings were used in this study.

3 MOISTURE BUDGET

Significant stratiform precipitation has been identified during the early phase of the WETAMC/TRMM-LBA experiment, dominated by the presence of the South American Convergence Zone (SACZ), with predominant winds from the west. As the experiment progressed, the SACZ decayed and the precipitation was predominantly convective, with winds predominant from the east (Rickenbach et al. 2001). The last period extended from mid-January to mid February. The last week of February was dominated by westerlies accompanied by an enhancement of the SACZ. According to Climanalise (1999) the SACZ was active during 6-18 January and after 19 February to end of the month.

3.1 SACZ and NSACZ events

Figure 2a shows the time series of the zonal wind observed during WETAMC/TRMM-LBA campaign based on soundings from ABRACOS-Rondonia (10°46'S-62°20'W). It was constructed by applying a 5-point running mean filter to 3-hourly sounding data. During the first weeks of January low-level winds were predominantly from west shifting to easterlies after January 19 and returned to westerlies after February 22. During three days, from 10-12 January, the winds shifted from westerlies to easterlies showing a little break at the westerlies regime. Figure 2b shows the time series of the 850 hPa zonal wind component from GEOS-2 DAS (Data Assimilation System) reanalysis from January to February 1999 at the grid point (10°S-62°30'W) near ABRACOS-Rondonia. The time series shown in Figure 2b, also constructed by applying a 5-point running mean filter to 6-hourly data, are in good agreement with the Figure 2a clearly showing the dominant westerly wind during the first days of January with a break from 10-12 January, and the shift to easterlies after January 19 remain until about February 22 when they shift to westerlies. The agreement between the observed data and DAO/NASA fields suggest that the assimilation products can be useful for studying these events.

The similarity between the observed data and DAO/NASA reanalysis becomes more clear in Figure 3 which shows the zonal winds at low-levels. A 3-day running mean is applied to the DAO/NASA analysis to smooth high-frequency variability and define low-level easterly and westerly winds periods (GEOS-2(3-day)). One major and one minor westerly wind episodes were characterized. The major westerly wind period began on 1st January and lasted until January 18 (Figure 3). The minor westerly wind episode began on February 22 and ended on February 28. The interim periods were defined as easterly regimes.

Composites of the OLR averaged over 1-18 Jan, 19-31 Jan, 1-21 Feb, and over 22-28 Feb, during the WETAMC/TRMM-LBA are shown in Figs 4 a, b, c, and d, respectively. As expected, the average over the first period (Fig. 4a) is characterized by strong convective activity over central tropical South America. The convection extends southeastward into the South Atlantic Ocean. This pattern is characteristic of SACZ events. Figure 4b shows the suppressed convection period featured much less deep convection, especially over southeastern Brazil where the SACZ is not as well organized as in earlier period. The following period (Fig. 4c) shows more activity but not enough to characterize as well defined a SACZ as the last period (Fig. 4d) where the SACZ extends from central Brazil southeastward across southeastern Brazil and the adjoining Atlantic Ocean.

The above results suggest that the variability of zonal wind component in the low-level at ABRACOS, confirmed by reanalysis from GEOS-2 DAS and composites of the OLR, can be separated into two distinct regimes: a) SACZ events that occurred during the first weeks of January and last week of February and b) NSACZ (No SACZ) events that take place during the last two weeks of January up to mid February when the SACZ is not present. With the purpose of simplifying the results and analysis, the whole period (January and February) was split and averaged for the two distinct regimes SACZ and NSACZ.

3.2 Vertically integrated moisture transport using GEOS-2 DAS

Intense moisture flux convergence over southeast and central Brazil characterize a SACZ event. This convergence extends over the adjacent south Atlantic ocean (Figure 5). Divergence can be observed over the eastern part of Brazil, northwestern of Argentina, Paraguay, southern of Bolivia and northern Chile. The NSACZ period is characterized by weakening of convergence over the southern Amazon, and southeast and central Brazil, and convergence in Argentina and Paraguay.

Figure 5 indicates the inversion of the climatological northerly moisture flux over northern Argentina and Paraguay to southerly, characterized by anomalous cyclonic circulation between 20^{o} and 25^{o}S, which is predominant during a SACZ event. A similar situation occurred over western central Amazon (near 10^{o}S-60^{o}W) with the occurrence of westerlies (easterlies) during the SACZ (NSACZ) event. During the SACZ (NSACZ) event the easterlies display an stronger (weaker) northern component over the northern Amazon characterizing an intensification of the moisture transport from the north.

As pointed out by Nogués-Peagle and Mo (1997) the subtropical high pressure system over the south Atlantic ocean shifts to the west during a NSACZ event contributing to the suppression of convergence over central/southeast Brazil observed during a SACZ event (Figure 5). Figure 6a shows strong low-level convergence, in particular over 15^{o}S, reflecting strong convection over this region during the SACZ event. This vertical circulation is also linked with strong tropical westerlies as evident from uq core (shading) at 850 hPa level and between 10^{o}-15^{o}S latitude. Strong convergence also occurred around the equator with strong easterlies (dark shading). Figure 6b shows moisture transport from the tropics to the subtropics during the NSACZ period. Strong convection occurred over Amazon basin (5^{o}S-5^{o}N), and over north of Argentina and Paraguay (25^{o}S-35^{o}S) during NSACZ event. Easterlies extended southward 5^{o}S (15^{o}S) in the SACZ (NSACZ) event turning to westerlies further south. This vertical cross section shows a meridional moisture transport with a dominant poleward direction in a latitude just to the south of the Amazon Basin (Fig. 6b). This is relevant to the analysis of the atmospheric branch of the hydrological cycle both over the Amazon and Prata Basin.

Figure 7 displays the vertical cross section of the mean moisture flux streamlines during the SACZ (Figure 7a) and NSACZ (Figure 7b) events at 15°S. The combination of a strong low-level jet bringing warm and moist air from the Atlantic ocean and Amazon to region around 50°W (Figure 7a) and low-level convergence (streamlines) produces a tendency for intense convection to occur at central/southeast Brazil that can be associated with the SACZ. The region of maximum northerly flux (Figure 7a) moves westward closer to the Andes Mountains during a NSACZ event (Figure 7b). As the transition takes place convection decays and a cyclonic circulation develops along the 63°W (streamlines) characterizing the moisture transport from the Amazon Basin toward mid-latitude South America, more specifically to northern Argentina, Paraguay and southern Brazil – Prata Basin (Figure 5b). Figueroa et al. (1995) and Gandu and Geisler (1991) have shown that during the wet season the effect of the Andes is to channel the low-level flow. Global analyses and some sparse observational data (Douglas et al. 2000; Marengo et al. 2001) suggest that there is a southward LLJ to the east of the Andes mountains that contributes to the meridional moisture transport from the Amazon Basin into the subtropical regions of South America and modulates convective outbreaks in those regions. Thissouthern LLJ has a structure similar to its North American counterpart (Nogués-Paegle and Mo 1997; Marengo et al. 2001).

3.3 Moisture flux transport between Amazon and Prata basin

Strong correlation can be observed between winds and specific humidity over Northern Argentina/Paraguay and the WETAMC/TRMM-LBA region (Figure 8). The period of westerlies (easterlies) flow over the Amazon region coincide with the southerly (northerly) flow over the Prata region (Figure 8a). The specific humidity over the Prata region shows low values during the southerly events shifting to high values during the northerly events (Figure 8b). The period of the southerly flow during the first weeks of January and last of February, coincides with the SACZ event. Northerly flow occurs during the NSACZ. This is in agreement with Nogués-Peagle and Mo (1997) where they support that when the SACZ is enhanced there is a weakening of the moisture transport to north Argentina, Paraguay and south/southeast of Brazil. On the other hand, the weakening of the SACZ (NSACZ event) is associated with the reinforcement of moisture transport to north Argentina, Paraguay and south/southeast of Brazil, with important consequences for the hydrological balance over the Prata Basin. Silva Dias (2000) used the RAMS mesoscale model and found similar results with intense low level jet (LLJ) during the time of NSACZ event (18-22 January, 27-28 January, 30 January until 03 February and 11-14 February).

4 SUMMARY AND CONCLUSIONS

The complex three-dimensional large-scale moisture transport over the Amazon and Prata basin , which was discussed in the previous sections, is summarized in Figure 9. This figure displays the vertically integrated moisture fluxes over the Amazon and Prata regions for the SACZ and NSACZ periods. The moisture fluxes are area weighted and the units are scaled to mm/day.

During the SACZ event (Figure 9a) strong convergence occurred over the Amazon with 55 mm/day of inflow. The strongest inflows are from the east (54 mm/day) and north (44 mm/day) and the weakest inflow occurs on the western portion of the southern boundary (4 mm/day). On the eastern side of the southern boundary there is outflow with moisture transport to central and southeast Brazil. This outflow (26 mm/day) is characteristic of the SACZ event. At the dotted line, in the Amazon box (Figure 9a), the fluxes are from the west at the bottom line and from the east at the top line (not shown). This also can be observed from Figure 5.

The convergence over the Amazon region, during NSACZ (Figure 9b) decreases by 46% resulting in an inflow of 31 mm/day. In fact, the inflow through the eastern boundary is almost 50% higher during NSACZ event, but the outflow at the western boundary is more than double during NSACZ when compared to SACZ period. The greatest moisture transport takes place at the eastern boundary (76 mm/day) followed by the northern boundary (34 mm/day), while the stronger outflow occurred at the western boundary (51 mm/day). The most important change in the flow occurred over the southern Amazon basin on the eastern side of the southern boundary, the weaker outflow characterizes the NSACZ event. On the western side of the southern boundary there is a shift from southerly to northerly flow from SACZ to NSACZ event.

The Prata basin has frequently been characterized as a net atmospheric moisture sink during summertime (Saulo et al. 2000). However, when the SACZ is present this region (Figure 9a) can be classified as a net moisture source. During the SACZ event the total moisture flux convergence over this region is negative (-4 mm/day) indicating outflow or divergence. In agreement with the results obtained by Nogués-Peagle and Mo (1997), the suppressed precipitation over the Prata basin is associated with enhanced SACZ event. When a NSACZ event takes place, there is enhanced moisture transport to Prata basin (44 mm/day) from the north and a net inflow of 5 mm/day . This flux at the northern boundary is as strong as the vertically integrated moisture flux from the north over the Amazon basin, during SACZ event. Enhanced northerly flow during NSACZ evidence the moisture transport from Amazon region to Prata basin, associated to Low Level Jet (LLJ). Robertson and Mechoso (2000) have shown that the Parana/Paraguay rivers (extending northward to near 15^{o}S,) are directly influenced by the SACZ and tend to swell during SACZ events. The Uruguay/Negro rivers (25^{o}-35^{o}S) to the south are influenced in the opposite sense (tend to ebb) through the dipole in vertical motion and possibly by accompanying variations in southward moisture transport by the LLJ east of the Andes.

The main characteristic over the Prata region is the inversion of the moisture flux in north-south boundaries from SACZ event to NSACZ event. This is in agreement with Min and Schubert (1997) that compared different assimilation products over this region for two selected extreme climate (drought and flood) events. Their vertically integrated moisture flux for the SACZ (NSACZ) event has the same characteristics to the drought (flood) event to this region. It is important to note that the enhanced inflow from north, during NSACZ, results in a enhanced outflow at the east boundary (32 mm/day) contributing to the moisture budget over the southern Brazil.

In conclusion, the low-level westerlies over the WETAMC/TRMM-LBA sites are associated with moisture convergence and enhanced rainfall in the Central/Southeastern Brazil, characteristic of a South Atlantic Convergence Zone – while the easterlies are linked with moisture convergence in Paraguay, and northern Argentina, with reduced convective activity in central/southeastern Brazil, and these patterns are similar to the SACZ and NSACZ episodes in the OLR data (Figure 4). Submonthly variations in the SACZ also can be linked to extreme climate anomalies such as droughts or flooding conditions over the Amazon and Prata basin.

Acknowledgments.

Parts of this project were supported by FAPESP and CNPq. DLH acknowledges a CAPES scholarship, and this work constitutes part of DLH PhD dissertation at University of São Paulo (USP). It is a pleasure to acknowledges the support of this work by Dr. Keneth Bergman, manager of Global Modeling and Analysis Program.

REFERENCES

Berri, G. J., and J. Inzunza B., 1993: The effect of the low-level jet on the poleward water vapour transport in the central region of South America. Atmos. Environment, 27:335-341.

Climanalise, 1999 – Boletim de Monitoramento e Analise Climatica, 14(1). Available from Centro de Previsão de Tempo e Estudos Climáticos, Rodovia Presidente Dutra km 40, 12630, Cachoeira Paulista – SP, Brasil (also available via internet at http://www.cptec.inpe.br/products/climanalise).

DAO, 1996: Algorithm theoretical basis document for Goddard Earth Observing System Data Assimilation System (GEOS DAS) with a focus on version 2. Data Assimilation Office, NASA's Goddard Space Flight Center, 310 pp.

Douglas, M.W., M. Pena, and R. Villarpando, 2000: Special observations of the low level flow over eastern Bolivia during the 1999 atmospheric mesoscale campaign. In Extended Abstracts of the 6th Int. Conf. On Southern Hemisphere Meteorology and Oceanography, 3-7 April 2000, Santiago, Chile. AMS Publ., 157-158.

Figueroa, S., P. Satyamurti, and P.L. Silva Dias, 1995: Simulation of the summer circulation over the South America region with Eta coordinate model. J. Atmos. Sci., 52: 573-584.

Gandu, A., and J. Geisler, 1991: A primitive equations model study of the effect of topography on the summer circulation over tropical South America. J. Atmos. Sci., 48: 1822-1836.

Garstang , M., and D. R. Fitzjarrald, 1999: Observations of surface to atmosphere interactions in the tropics, 1st ed., 405 pp., Oxford University Press, New York.

Kodama, Y., 1992: Large-scale common features of subtropical precipitation zones (the Baiu frontal zone, the SPCZ, and the SACZ). Part I: Characteristics of subtropical zones. J. Meteo. Soc. Japan, 70: 813-835.

Kodama, Y., 1993: Large-scale common features of subtropical precipitation zones (the Baiu frontal zone, the SPCZ, and the SACZ). Part II: Conditions of the circulations for generating STCZs. J. Meteo. Soc. Japan, 71: 581-610.

Labraga, J. C., O. Frumento, and M. Lopez, 2000: The atmospheric water vapor cycle in South America and the tropospheric circulation. J. Climate, 13: 1899-1915.

Lenters, J.D., and K.H. Cook, 1999: Summertime precipitation variability over South America: Role of the large-scale circulation. Mon. Wea. Rev., 127: 409-431.

Liebmann, B., and C. A. Smith, 1996: Description of complete (interpolated) outgoing longwave radiation data set. Bull. Amer. Meteor. Soc., 77: 1275-1277.

Liebmann, B., G. Kiladis, J. Marengo, and T. Ambrizzi, 1999: Submonthly convective variability over South America and the South Atlantic Convergence Zone. J. Climate, 12:1877-1891.

Marengo, J, 2000: Characteristics and variability of the atmospheric water balance of the Amazon Basin. In Extended Abstracts of the 6th Int. Conf. On Southern Hemisphere Meteorology and Oceanography, 3-7 April 2000, Santiago, Chile. AMS Publ., 284-285.

Marengo, J.A., M.W. Douglas, and P.L. Silva Dias, 2001: Towards a identification of the South American low-level jet east of the Andes during the LBA-TRMM and LBA-WET AMC campaign of the summer of 1999. J. Geophys. Res. (submitted).

Min, W., and S. Schubert, 1997: The climate signal in regional moisture fluxes: A comparison of three global data assimilation products. J. Climate, 10: 2623-2642.

Mo, K. C., and R. W. Higgins, 1996: Large scale atmospheric moisture transport as evaluated in the NCEP/NCAR and the NASA/DAO reanalyses. J. Climate, 9: 1531-1545.

Nogués-Peagle, J., and K. C. Mo, 1997: Alternating wet and dry conditions over South America during summer. Mon. Wea. Rev., 125: 279-291.

Nogués-Peagle, J., K. C. Mo, and J. Peagle, 1998: Predictability of the NCEP-NCAR reanalysis model during austral summer. Mon. Wea. Rev., 126: 3135-3152.

Rickenbach, T., R. Nieto Ferreira, J. Halverson, and M. A. F. Silva Dias 2001: Modulation of the convection in the southwestern Amazon basin by extratropical stationary fronts. J. Geophys. Res., (accepted).

Robertson, A.W., and C. Mechoso, 2000: Interannual and interdecadal variability of the South Atlantic Convergence Zone. Mon. Wea. Rev., 128:2947-2957.

Saulo, A.C., M. Nicolini, and S.C. Chou, 2000: Model characterization of the South American low-level flow during the 1997-1998 spring-summer season. Climate Dynamics, 16:867-881.

--, --, and Pfaendtner, 1993: An assimilated dataset for earth science applications. Bull. Amer. Meteor. Soc. 74, 2331-2342.

--, H. M. Helfand, C. Wu, and W. Min, 1998: Subseasonal variations in warm-season moisture transport and precipitation over the Central and eastern United States. J. Climate, 11: 2530-2555.

Seluchi, M. E., and Marengo, J. A. 2000. Tropical-midlatitude exchange of air masses during summer and winter in South America: Climatic aspects and examples of intense events. Int. J. Climatol., 20:1167-1190.

Shay-El, Y., P. Alpert, and A. da Silva, 1999: Reassessment of the moisture source over the Sahara Desert based on NASA reanalysis. J. Geophys. Res., 104:2015-2030.

Silva Dias, P.L., 2000: The role of latent heat released in the dynamics of the LLJ's along the Andes. In Extended Abstracts of the 6th Int. Conf. On Southern Hemisphere Meteorology and Oceanography, 3-7 April 2000, Santiago, Chile. AMS Publ., 163-164.

Silva Dias, M. A. F., A. J. Dolman, P. L. Silva Dias, S. Rutledge, E. J. Zipser, G. Fisch, P. Artaxo, A. Manzi, J. Marengo, C. Nobre, and P. Kabat, 2000: Rainfall and surface process in Amazonia during the WETAMC/LBA – An overview. In Extended Abstracts of the 6th Int. Conf. On Southern Hemisphere Meteorology and Oceanography, 3-7 April 2000, Santiago, Chile. AMS Publ., 249-250.

--, S. Rutledge, P. Kabat, P. L. Silva Dias, C. Nobre, G. Fisch, A. J. Dolman, E. Zipser, M. Garstang, A. Manzi, J. D. Fuentes, H. Rocha, J. Marengo, A. Plana-Fattori, L. Sa, R. Alvala, M. o. Andreae, P. Artaxo, R. Gielow, L. Gatti, 2001: Clouds and rain process in a biosphere atmosphere interaction context in the Amazon region. J. Geophys. Res. (submitted).

FIGURE CAPTIONS

Figure 1 – Map of South America with the experimental area in the State of Rondonia. The enhanced map shows the WETAMC/TRMM-LBA sites with the instrumentation deployed. The small colored squares are the GTS sites used by GEOS-2 reanalysis. The shaded in the background denote land surface elevation (m).

Figure 2 – Time series of the zonal wind component observed at ABRACOS (10°46'S-62°20'W) site during WETAMC/LBA-TRMM campaign (January-February/1999) in Ji-Parana (a) and from GEOS-2 dataset at 10°S-62°30'W (b). Units are m/s.

Figure 3 – Time series of the zonal wind component at 850 hPa during WETAMC/LBA-TRMM campaign for ABRACOS at 10°46'S-62°20'W (solid line), GEOS-2 dataset at 10°S-62°30'W (dashed line), and three days running mean GEOS-2. Units are m/s.

Figure 4 – A composite of the Outgoing Long wave Radiation (OLR) averaged over a) 1-18 Jan 1999, b) 19-31 Jan 1999, c) 1-21 Feb 1999, and d) 22-28 Feb 1999, during the WETAMC/TRMM-LBA. Image provided by the NOAA-CIRES Climate Diagnostics Center, Boulder, Colorado, USA, from their Web site at http://www.cdc.noaa.gov/. Units are W/m2.

Figure 5 – Vertically integrated regional moisture flux (streamline) and moisture flux divergence (shaded) for (a) SACZ period and (b) NSACZ period from GEOS-2 dataset. Divergence units of mm/day.

Figure 6 – Vertical cross section of the mean moisture flux streamlines (vq,wq) along longitude 60°W, and uq in shading, calculated from GEOS-2 dataset. SACZ (a) and NSACZ (b). A shading bar, in units of (g/kg)/(m/s), is at bottom of the figure.

Figure 7 – Vertical cross section of the mean moisture flux streamlines (uq,wq) along latitude 15°S, and vq in shading, calculated from GEOS-2 dataset. SACZ (a) and NSACZ (b). A shading bar, in units of (g/kg)/(m/s), is at bottom of the figure.

Figure 8 – Time series from GEOS-2 dataset at 850 hPa for (a) zonal wind at 10°S-62°30'W (dashed line) and meridional wind at 20°S-60°W (solid line). Panel (b) show the specific humidity at 10°S-62°30'W (dashed line) and at 20°S-60°W (solid line). The units are (m/s) for (a) and (g/kg) for (b).

Figure 9 – Vertically integrated moisture fluxes across the lateral boundaries and the area averaged vertically integrated moisture flux convergence over the Amazon basin, and over the Prata basin for (a) SACZ and (b) NSACZ period using GEOS-2 dataset. Units are mm/day.

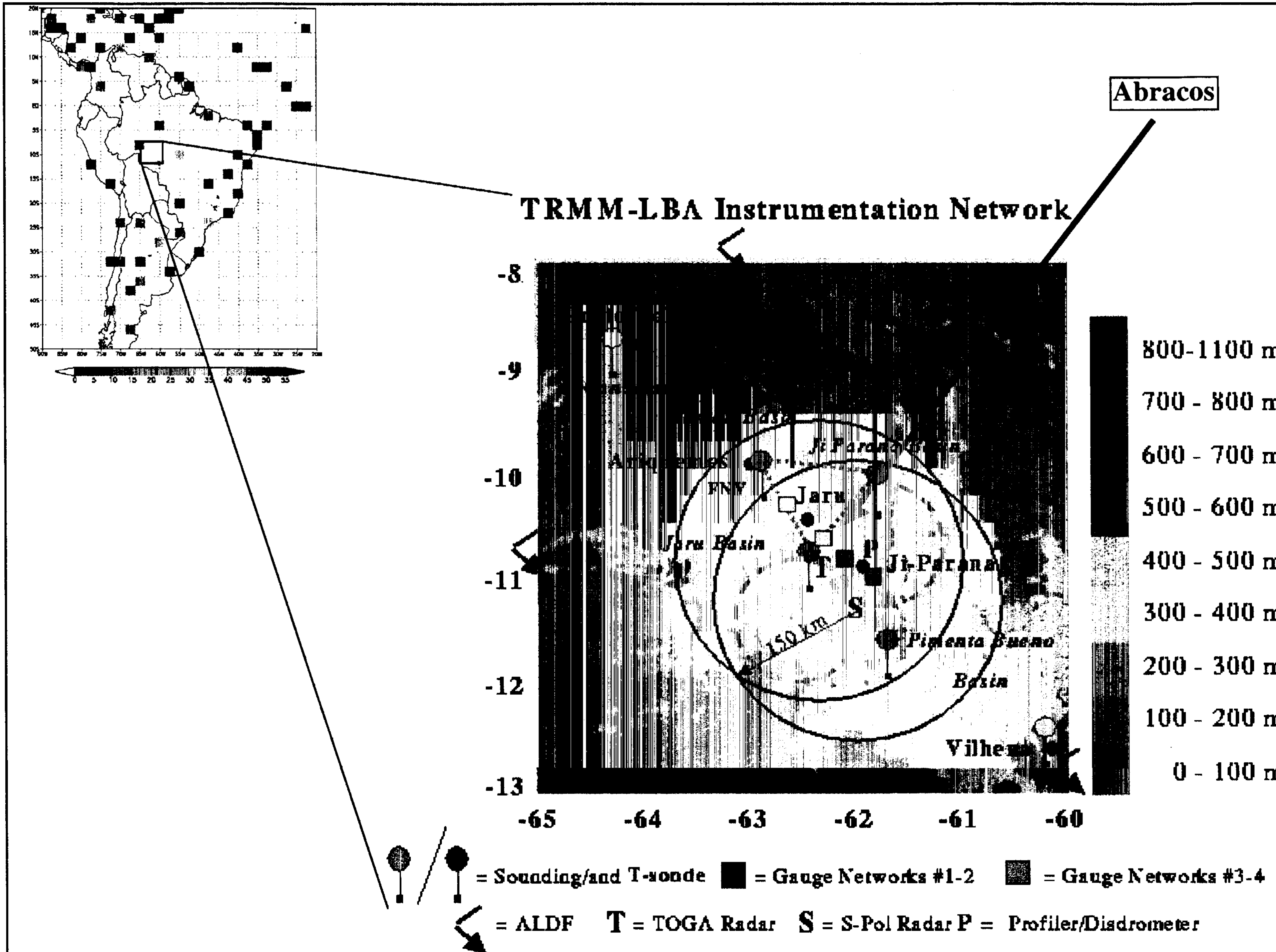

TRMM-LBA Instrumentation Network
Abracos
Jaru
FNV
Jaru Basin
Ji-Parana
Pimenta Bueno
Basin
Vilhe
150 km
S
T
P
-8
-9
-10
-11
-12
-13
-65
-64
-63
-62
-61
-60
800-1100 m
700 - 800 m
600 - 700 m
500 - 600 m
400 - 500 m
300 - 400 m
200 - 300 m
100 - 200 m
0 - 100 m
= Sounding/and T-sonde
= Gauge Networks #1-2
= Gauge Networks #3-4
= ALDF
T = TOGA Radar
S = S-Pol Radar
P = Profiler/Disdrometer

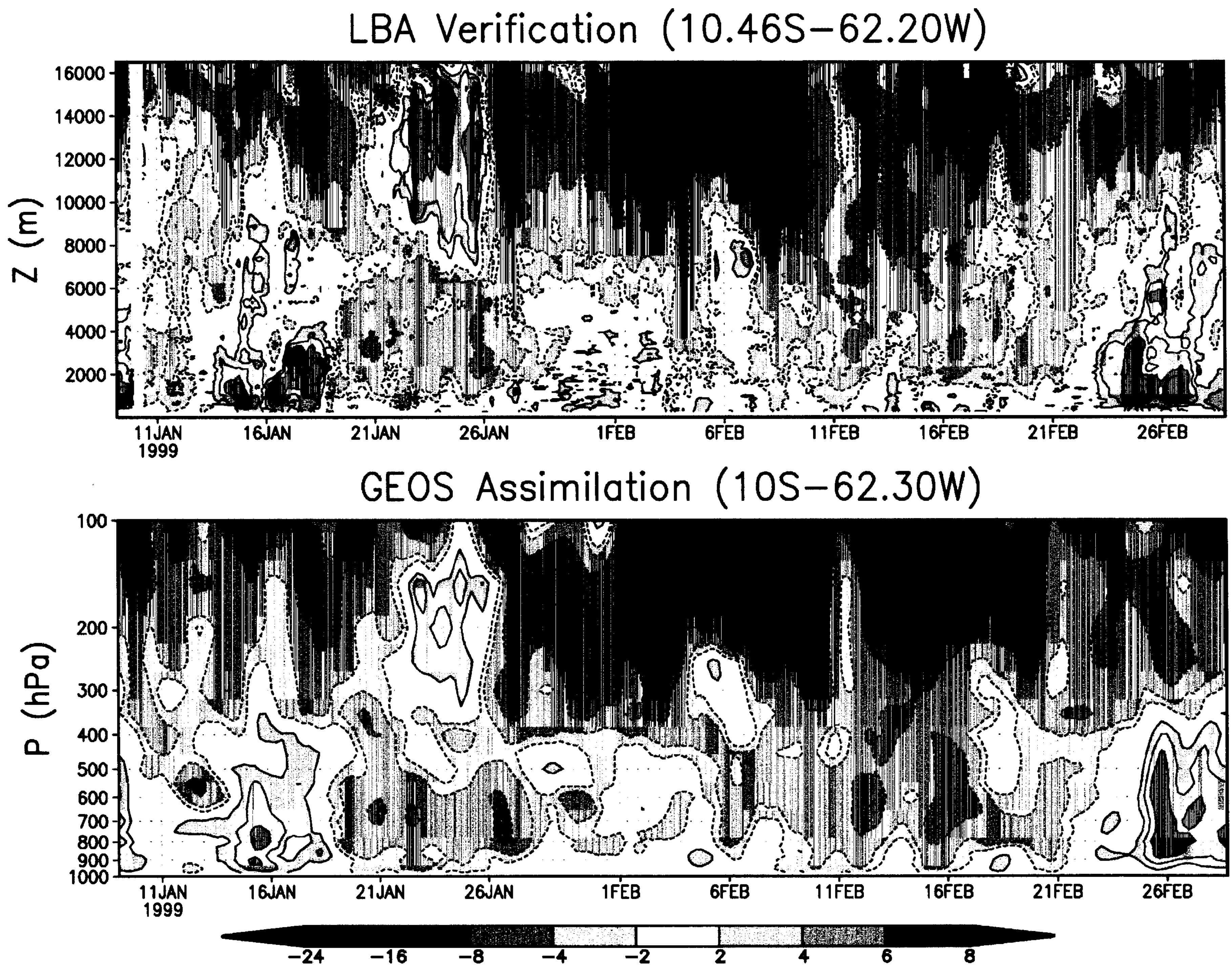
LBA Verification (10.46S−62.20W)
Z (m)
16000
14000
12000
10000
8000
6000
4000
2000
11JAN 1999
16JAN
21JAN
26JAN
1FEB
6FEB
11FEB
16FEB
21FEB
26FEB
GEOS Assimilation (10S−62.30W)
P (hPa)
100
200
300
400
500
600
700
800
900
1000
11JAN 1999
16JAN
21JAN
26JAN
1FEB
6FEB
11FEB
16FEB
21FEB
26FEB
−24
−16
−8
−4
−2
2
4
6
8

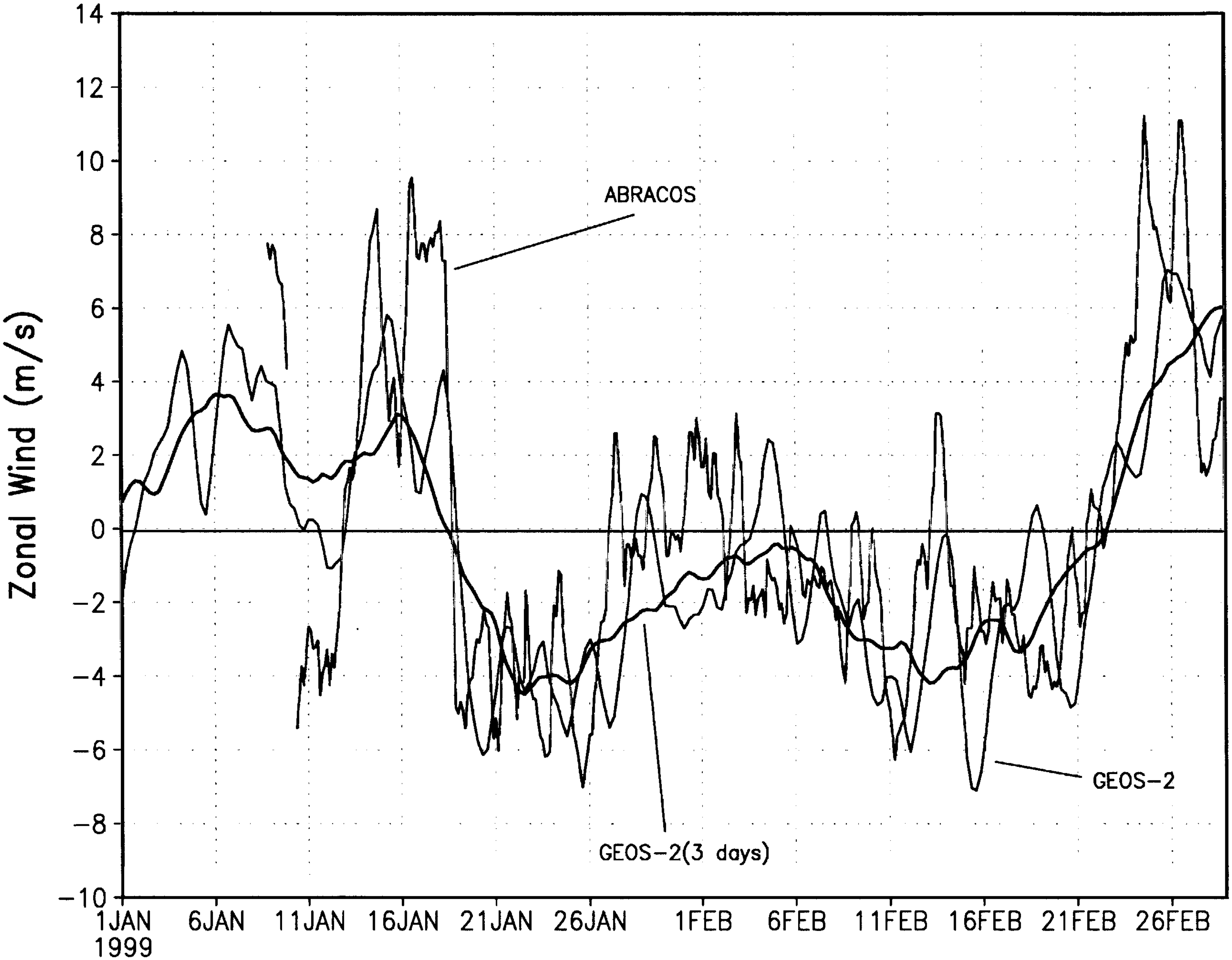
Zonal Wind (m/s)
14
12
10
8
6
4
2
0
−2
−4
−6
−8
−10
1JAN
1999
6JAN
11JAN
16JAN
21JAN
26JAN
1FEB
6FEB
11FEB
16FEB
21FEB
26FEB
ABRACOS
GEOS−2(3 days)
GEOS−2

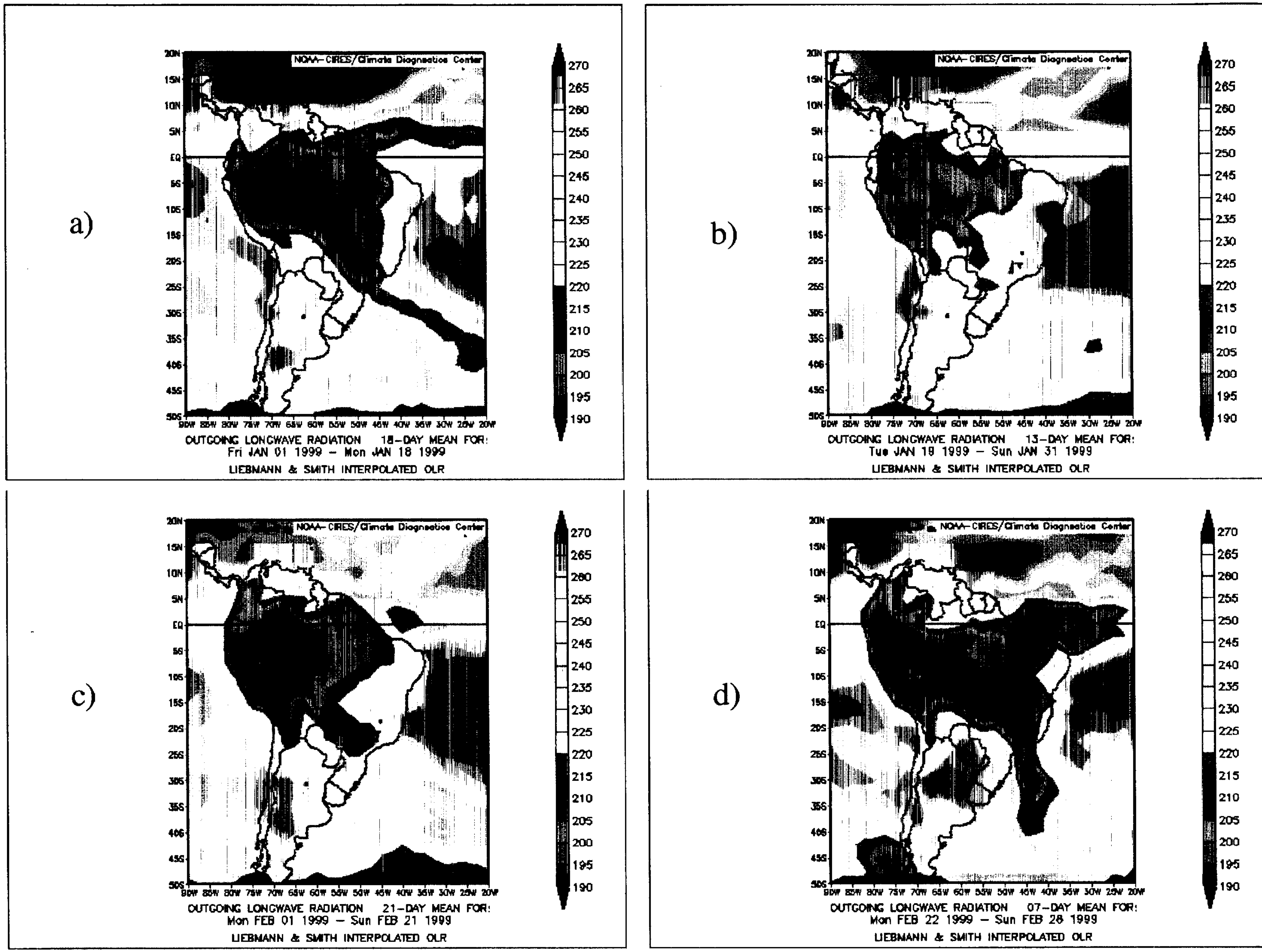
a)
NOAA-CIRES/Climate Diagnostics Center
OUTGOING LONGWAVE RADIATION 18-DAY MEAN FOR:
Fri JAN 01 1999 – Mon JAN 18 1999
LIEBMANN & SMITH INTERPOLATED OLR
b)
NOAA-CIRES/Climate Diagnostics Center
OUTGOING LONGWAVE RADIATION 13-DAY MEAN FOR:
Tue JAN 19 1999 – Sun JAN 31 1999
LIEBMANN & SMITH INTERPOLATED OLR
c)
NOAA-CIRES/Climate Diagnostics Center
OUTGOING LONGWAVE RADIATION 21-DAY MEAN FOR:
Mon FEB 01 1999 – Sun FEB 21 1999
LIEBMANN & SMITH INTERPOLATED OLR
d)
NOAA-CIRES/Climate Diagnostics Center
OUTGOING LONGWAVE RADIATION 07-DAY MEAN FOR:
Mon FEB 22 1999 – Sun FEB 28 1999
LIEBMANN & SMITH INTERPOLATED OLR
20N 15N 10N 5N EQ 5S 10S 15S 20S 25S 30S 35S 40S 45S 50S
90W 85W 80W 75W 70W 65W 60W 55W 50W 45W 40W 35W 30W 25W 20W
270 265 260 255 250 245 240 235 230 225 220 215 210 205 200 195 190

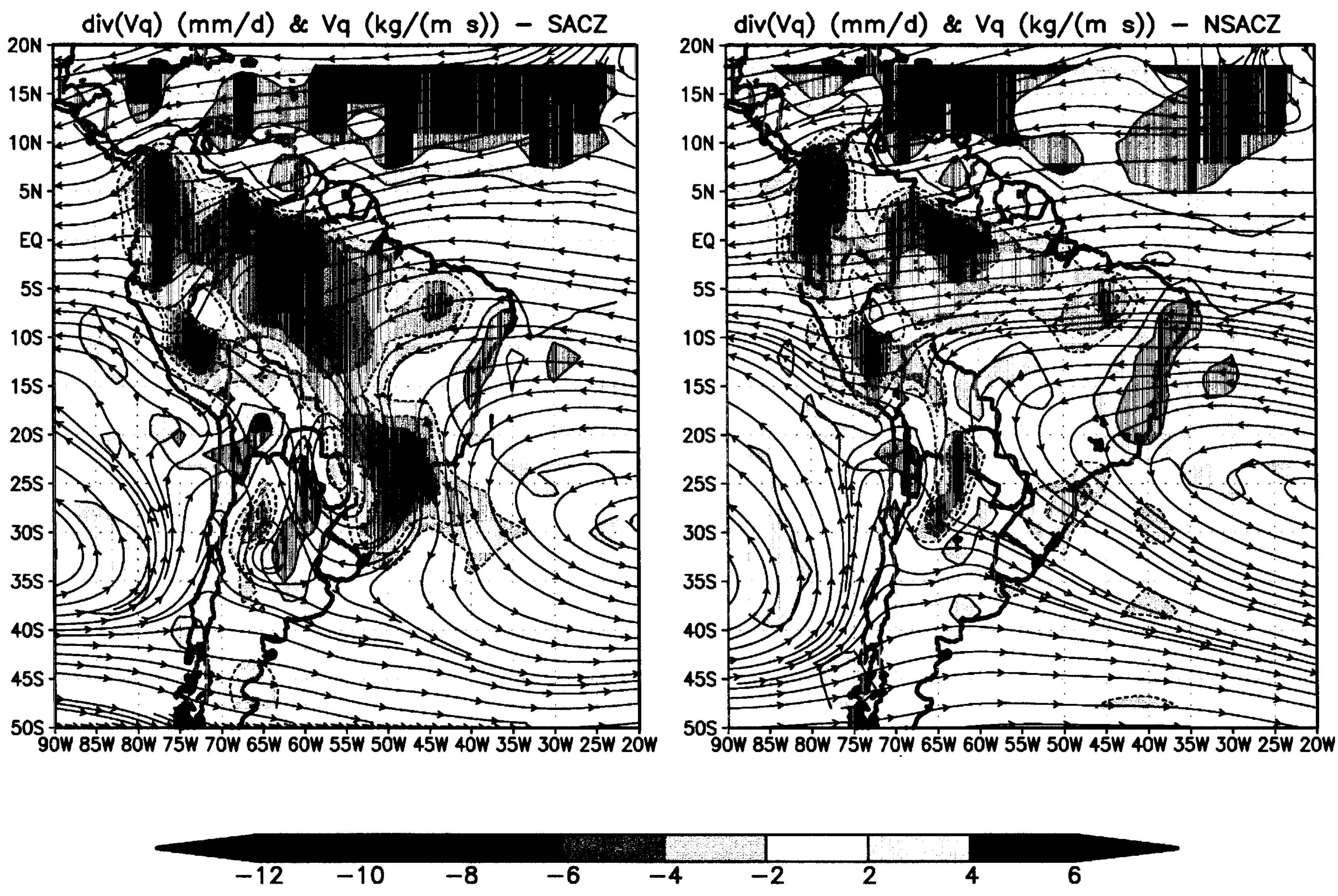

div(Vq) (mm/d) & Vq (kg/(m s)) - SACZ
div(Vq) (mm/d) & Vq (kg/(m s)) - NSACZ
20N
15N
10N
5N
EQ
5S
10S
15S
20S
25S
30S
35S
40S
45S
50S
90W 85W 80W 75W 70W 65W 60W 55W 50W 45W 40W 35W 30W 25W 20W
−12 −10 −8 −6 −4 −2 2 4 6

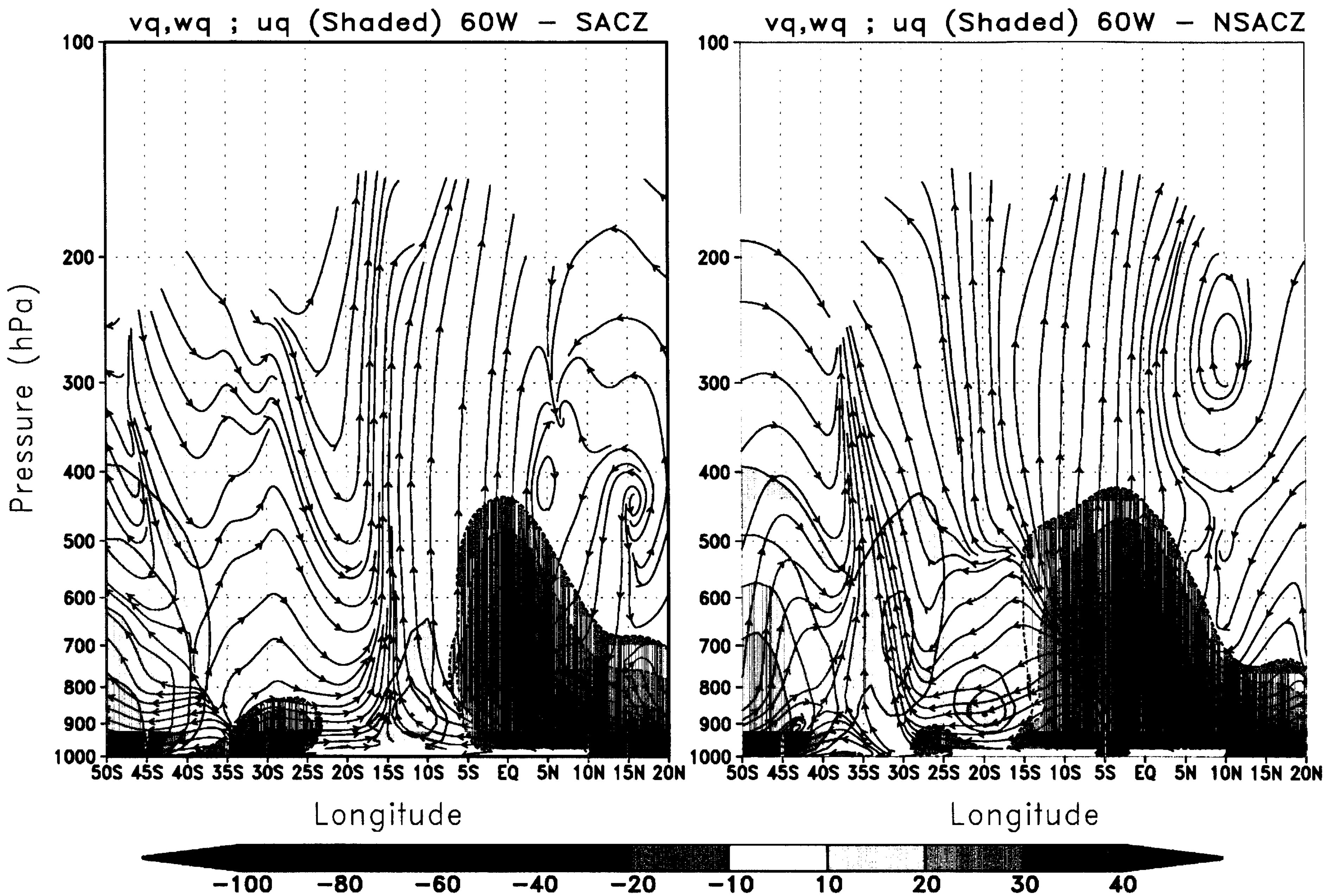

vq,wq ; uq (Shaded) 60W – SACZ
vq,wq ; uq (Shaded) 60W – NSACZ
Pressure (hPa)
100
200
300
400
500
600
700
800
900
1000
50S 45S 40S 35S 30S 25S 20S 15S 10S 5S EQ 5N 10N 15N 20N
Longitude
−100 −80 −60 −40 −20 −10 10 20 30 40

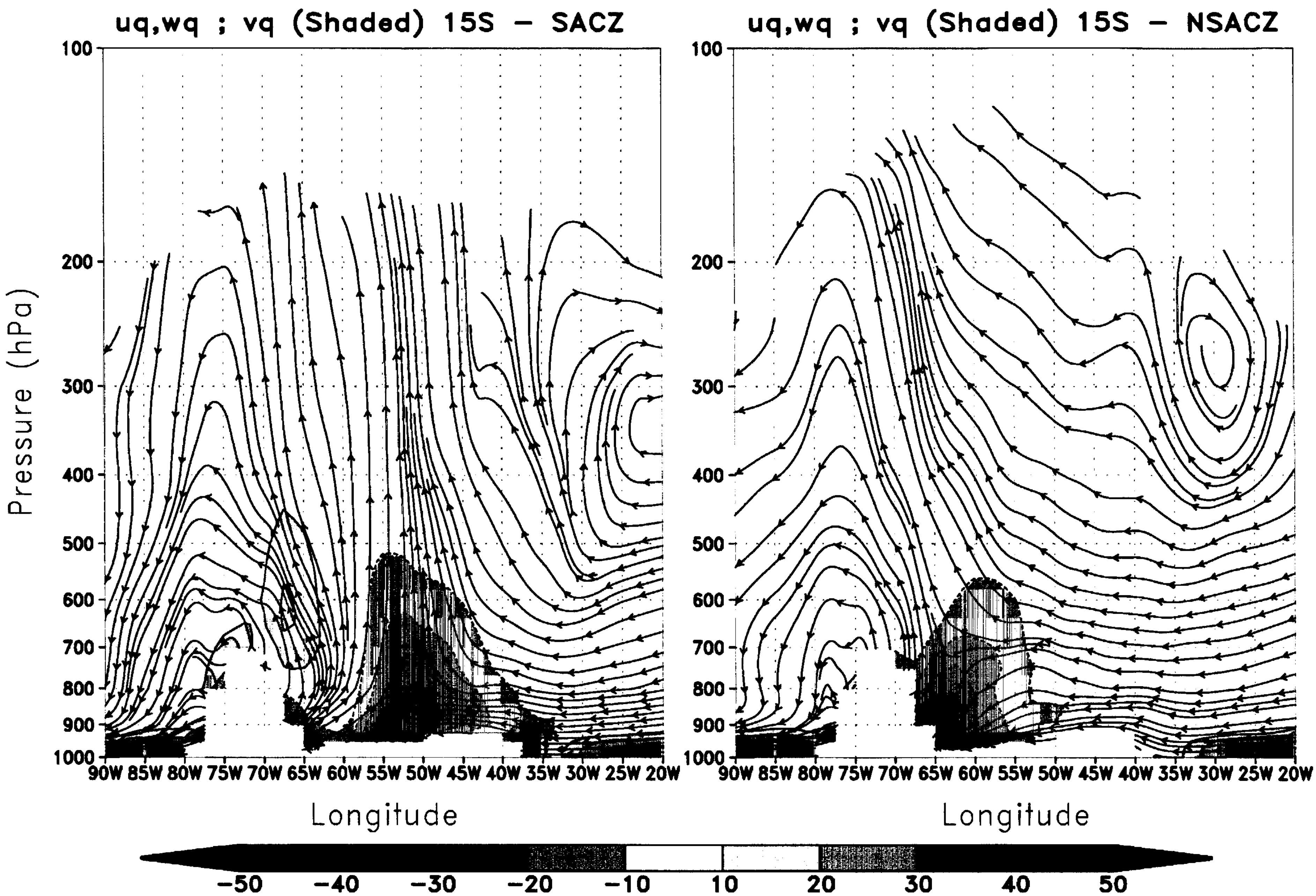
uq,wq ; vq (Shaded) 15S - SACZ
uq,wq ; vq (Shaded) 15S - NSACZ
Pressure (hPa)
100
200
300
400
500
600
700
800
900
1000
90W 85W 80W 75W 70W 65W 60W 55W 50W 45W 40W 35W 30W 25W 20W
Longitude
-50 -40 -30 -20 -10 10 20 30 40 50

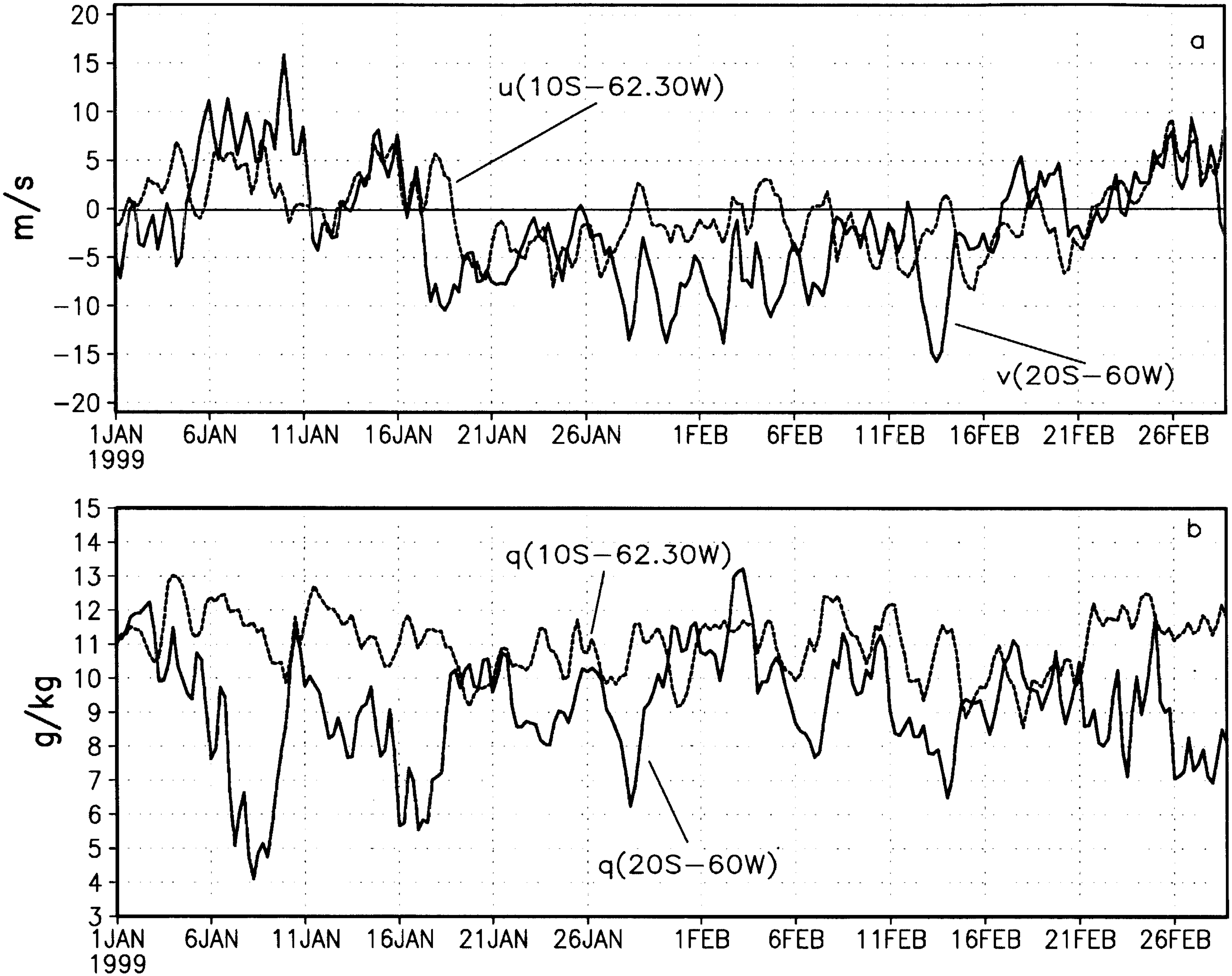

a
u(10S−62.30W)
v(20S−60W)
m/s
20
15
10
5
0
−5
−10
−15
−20
1JAN
1999
6JAN
11JAN
16JAN
21JAN
26JAN
1FEB
6FEB
11FEB
16FEB
21FEB
26FEB
b
q(10S−62.30W)
q(20S−60W)
g/kg
15
14
13
12
11
10
9
8
7
6
5
4
3
1JAN
1999
6JAN
11JAN
16JAN
21JAN
26JAN
1FEB
6FEB
11FEB
16FEB
21FEB
26FEB

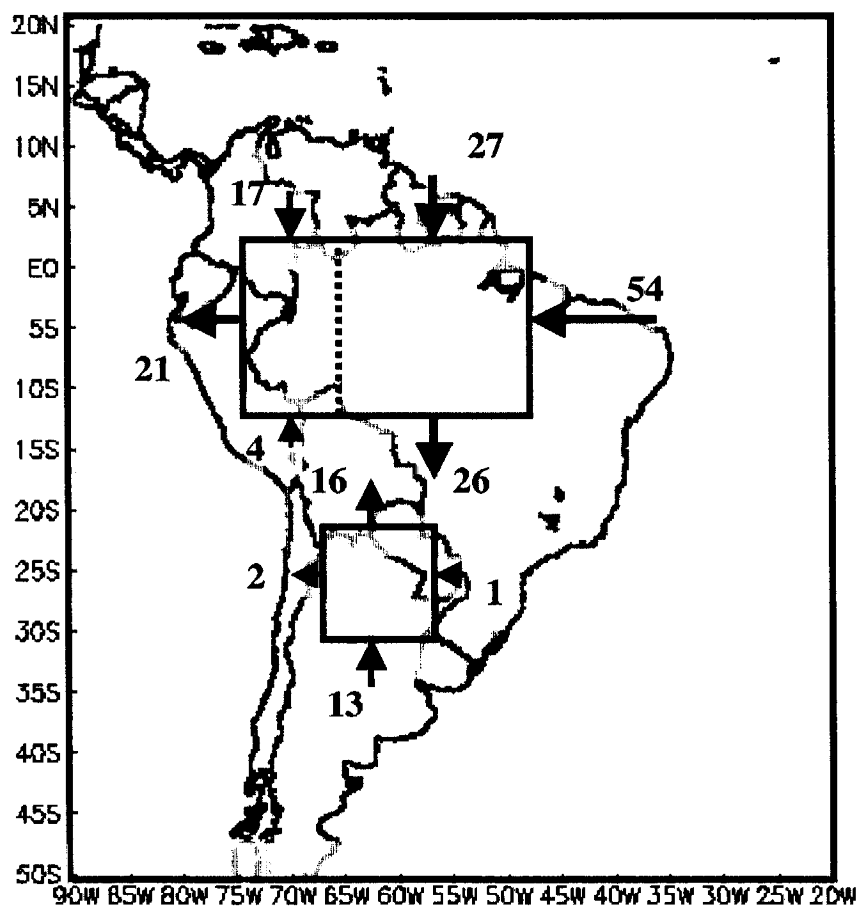

Total flux convergence

Amazon: 55 inflow   Prata: -4 outflow

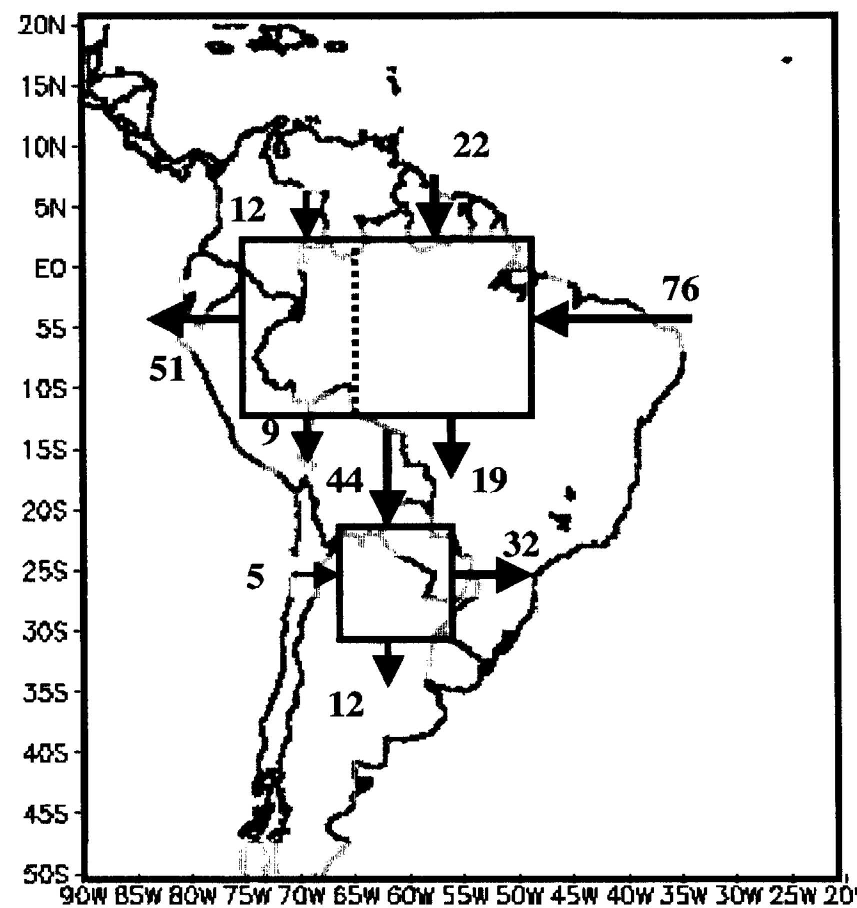

Total flux convergence

Amazon: 31 inflow   Prata: 5 inflow